# Inactivation of the Wnt/β-catenin signaling contributes to the epithelial barrier dysfunction induced by sodium oxalate in canine renal epithelial cells

**Yun Ji**
China Agricultural University
**Shuting Fang**
China Agricultural University
**Ying Yang**
China Agricultural University
**Zhenlong Wu** ( bio2046@hotmail.com )
China Agricultural University https://orcid.org/0000-0001-9700-8874

**Research**

**Keywords:** Barrier function, Canine, Cell proliferation, Oxalate, Renal epithelial cell, Wnt/β-catenin

**Posted Date:** March 3rd, 2021

**DOI:** https://doi.org/10.21203/rs.3.rs-253975/v1

## Abstract

# Background

Nephrolithiasis (also known as renal stones) is a common disease condition in companion animals, including dogs and cats. Dysfunction of renal tubular epithelial cells involves in the pathogenesis of renal stones. However, a functional role of Wnt/β-catenin signaling and its contribution to nephrolithiasis remains unknown.

# Results

In the present study, we found that Mardin-Darby canine kidney (MDCK) cells treated with sodium oxalate resulted in reduced cell proliferation and migration, which was associated with the G0/G1 phase arrest of cell cycle progression. In addition, sodium oxalate exposure led to decreased transepithelial electrical resistance (TEER) and increased paracellular permeability. The deleterious effect of sodium oxalate on epithelial barrier function was related to decreased protein abundances of claudin-1, occludin, zonula occludens (ZO)-1, ZO-2 and ZO-3. Of note, protein levels of p-β-catenin (Ser552) in MDCK cells were repressed by sodium oxalate, indicating an inhibitory effect on the Wnt/β-catenin signaling. Intriguingly, SB216763, a GSK-3β inhibitor, enhanced the expression p-β-catenin (Ser552), and protected against epithelial barrier dysfunction in sodium oxalate-treated MDCK cells.

# Conclusion

Taken together, our results revealed a critical role of Wnt/β-catenin signaling on the epithelial barrier function of MDCK cells. Activation of Wnt/β-catenin signaling might be an potentially therapeutic target for the treatment of renal stones in animals.

## Introduction

Nephrolithiasis, also known as renal stones, is a complicated pathological condition in which crystals or stones are deposited inside the kidney [1]. Nephrolithiasis has become a frequent health problem in humans and animals. It was generally believed that renal stones formed by calcium oxalate is the second most prevalent type of nephrolithiasis occurred in companion animals (e.g. dogs and cats) [2, 3]. Intake of high-level oxalate has been a risk factor expediting the formation of calcium oxalate stone. Also, exposure of oxalate or calcium oxalate crystals induces cellular injury and impairment of the renal tubular epithelium [4]. In response to renal injury, epithelial cells undergo proliferation for regeneration and tissue repair. Of particular note, the epithelial tight junction proteins, such as zonula occludens (ZOs), occludin, claudins, and junctional adhesion molecules (JAMs), are critical determinant for the paracellular transport in renal tubular epithelial cells [5], which may be disrupted following the renal stone-induced

renal damage. Hence, exploring the mechanism related to function of the renal epithelial barrier is of significance for prevention or treatment of nephrolithiasis in humans and companion animals.

The canonical Wnt/β-catenin signaling is critical for embryonic development, wound-healing, and malignancies due to implication in a myriad of biological processes, such as proliferation, differentiation, migration, polarity, and cell death [6, 7]. In the absence of Wnt ligands, the transcriptional activity is maintained at a lower level due to the β-catenin destruction complex, which is composed of the scaffold protein Axin, adenomatous polyposis coli protein APC, and two kinases, including glycogen synthase kinase-3 (GSK-3) and casein kinase 1 (CK1) [8]. In response to Wnt ligands, β-catenin the activity of destruction complex is inhibited and leads to accumulation of β-catenin, which is subsequently translocation to the nucleus, and activates downstream targets by binding to and through interacting with the T cell factor (TCF)/lymphoid enhancer-binding factor (LEF) family of transcription factors [9]. Over the past years, Wnt/β-catenin signaling has been identified to be involved in the modulation of multiple kidney diseases [10–12]. Despite these findings, the functional role of Wnt/β-catenin signaling and its contribution to oxalate-induced disorder in renal epithelial barrier remains unknown. In the present study, Mardin-Darby canine kidney (MDCK) cells were incubated with or without sodium oxalate to induce cellular damage. Cell viability, cell cycle profile, proteins implicated in barrier function, as well underlying mechanisms were determined .

# Materials And Methods

### Reagents

Dulbecco's modified eagle medium (DMEM), $Ca^{2+}$-free DMEM, and fetal bovine serum (FBS) were purchased from Gibco (Carlsbad, CA, USA). Sodium oxalate, trypan blue, propidium iodide (PI), and FITC-dextran (20 kDa) were bought from Sigma-Aldrich (St. Louis, MO, USA). TRIzol Reagent was obtained from Mei5 Biotechnology (Beijing, China). cDNA Synthesis SuperMix was produced by Yeasen Biotech (Shanghai, China). SYBR Green qPCR Mix was purchased from Aidlab Biotechnologies (Beijing, China). LDH Release Assay Kit and EdU Cell Proliferation Kit were obtained from Beyotime Biotechnology (Shanghai, China). Annexin V-FITC Apoptosis Detection Kit was purchased from JIAMAYBIOTECH (Beijing, China). Antibodies against claudin-1, occludin, ZO-1, ZO-2, and ZO-3 were products of Sangon Biotech (Shanghai, China). Antibodies against cleaved-caspase-3, β-catenin, phospho-β-catenin (Ser552) were obtained from Cell Signaling Technology (Beverly, MA, USA). Antibodies against PARP1 and β-actin were purchased from Santa Cruz Biotechnology (Santa Cruz, CA, USA). SB216763 was obtained from Tocris Bioscience (Bristol, Avon, UK).

### Cell culture

MDCK cells, a canine-derived renal epithelial cell line, were cultured in DMEM medium supplemented with 10% FBS and 1% penicillin-streptomycin at 37 °C in a humidified 5% $CO_2$ atmosphere. Cells were passaged once 80-90% confluence was reached.

### Trypan blue assay

MDCK cells were seeded in 6-well plates ($6\times10^4$ cells per well). As cells expanded to 70% confluency, they were treated with 0, 0.5, 1, 2, 4 mmol/L sodium oxalate for 24 h. Cells were harvested with 0.25% trypsin-EDTA and then incubated with 0.4% trypan blue solution for 2 min at room temperature. Using an inverted microscope (Olympus, Japan), the stained cells were observed and counted with hemocytometer.

### Scratch assay

Briefly, MDCK cells were seeded in 6-well plates, which labeled by markers for wound location. Once confluence reached >90%, the cell monolayer was scratched by using 200 μL sterile pipette tips. The magnitude and direction of the force applied to pipette tips was as consistent as possible. After washing 3 times with PBS to remove debris, cells were subsequently treated with $Ca^{2+}$-free medium containing various concentration of sodium oxalate. Cell migration was observed under an inverted microscope with images acquisition device at 12 and 24 h, respectively. Wound areas were calculated using the Image J software (NIH, USA).

### LDH release determination

Concentration of lactate dehydrogenase (LDH) in supernatant was measured using the LDH Release Assay Kit following the manufacturer's instructions. MDCK cells were seeded onto 96-well plates (3000 cells per well) and then incubated with FBS-free medium containing various concentrations of sodium oxalate for 24 h. The supernatant and working solution were transferred into new 96-well plates by a ratio of 2:1 and incubated for 30 min at room temperature in the dark. Subsequently, the absorbance was measured at 490 nm using a SpectraMax M3 Multi-Mode Microplate Reader (Molecular Devices, USA).

### Cell cycle analysis

After a 6-h starvation in FBS-free medium, MDCK cells were incubated with various concentrations of sodium oxalate for 24 h. Cells were collected and washed twice with ice-cold PBS, followed by 70% ethanol fixation at -20 °C overnight. The ethanol was removed completely by washing twice with PBS. After incubation with 100 μg/mL RNase A for 20 min, cells were stained with 50 μg/mL propidium iodide (PI) for 30 min at room temperature in the dark. The fluorescence intensity of cells was analyzed by the CytoFLEX flow cytometer (Beckman Coulter, USA), and the data were presented as percentages of cells in G1, S and G2/M phases by the CytExpert software (Beckman Coulter, USA).

### 5-Ethynyl-2'-deoxyuridine (EdU) assay

The effect of sodium oxalate on cell proliferation was further confirmed by using the EdU Cell Proliferation Kit, following the protocol provided by manufacturer. MDCK cells were seeded in 24-well plates with a density of $3\times10^4$ cells/well and treated with sodium oxalate for 24 h. Then, prewarmed 5-ethynyl-2'-deoxyuridine (EdU) solution was added and the plates were incubated for 2 h in an incubator at

37 °C, flowing which the cells were stained by Hoechst 33342 (5 μg/mL) for 10 min away from light. The stained cells were observed and photographed under a fluorescence microscope (Zeiss, Germany).

### Quantitative real-time PCR (RT-qPCR)

After treatment with sodium oxalate for 24 h, MDCK cells were subjected to total RNA extraction by using the TRIzol Reagent and reverse transcribed into cDNA by means of the cDNA Synthesis SuperMix according to the manufacturer's instructions. Quantitative real-time PCR was performed with the SYBR Green qPCR Mix using the ABI 7500 real time-PCR system (Life Technologies, USA). Primer sequences used in this experiment are listed in **Supplemental Table 1**. *GAPDH* was used as a reference gene in the calculation of the relative expression level of a target gene by the $2^{-\Delta\Delta CT}$ method.

### Monolayer transepithelial electrical resistance determination

Briefly, MDCK cells were seeded in the apical side of transwell inserts (polycarbonate membrane; membrane area, 0.33 $cm^2$; pore size, 0.4 mm) in 24-well plates with a density of $5\times10^4$ cells per well. The transepithelial electrical resistance (TEER) of cells was measured by using a Millicell ERS-2 Volt-Ohm Meter (Millipore, USA) every day. After the values of TEER reaching a plateau, cells were challenged with 0, 0.5, 1, 2, 4 mmol/L of sodium oxalate. Within 48 h after treatment, TEER was determined and recorded every 12 h.

### Monolayer paracellular permeability measurement

As described above, the monolayer cellular barrier was established. 1 mg/mL FITC-dextran and sodium oxalate were added into the apical side of monolayer. At 0, 12, 24 and 48 h, the fluorescence intensity of medium obtained from the basolateral side was measured by using the SpectraMax M3 Multi-Mode Microplate Reader at the excitation and emission wavelength of 490 and 520nm, respectively.

### Western blot analysis

MDCK cells incubated with sodium oxalate were collected for protein extraction by using radioimmunoprecipitation assay (RIPA) lysis buffer. The concentration of protein was determined by bicinchoninic acid (BCA) assay. 25 mg denatured protein of each sample was separated by 10% sodium dodecyl sulphate-polyacrylamide gel electrophoresis (SDS-PAGE) gels, and then transferred to polyvinylidene difluoride (PVDF) membranes. The membranes were blocked by 5% nonfat milk for 1 h at 25 °C, subsequently incubated with primary antibodies (1: 2000) overnight at 4 °C. After that, the membranes were incubated with appropriate secondary antibodies (1:5000) for 1 h at 25 °C. The bands of target protein were visualized by the Image Quant LAS 4000 mini system (GE Healthcare, Sweden) after incubation with the enhanced chemiluminescence (ECL) reagent. The intensity of blots was measured by Image J software (NIH, USA) and normalized to GAPDH. All results indicated as the relative value of the control group.

### Statistical analysis

Data were represented as mean ± SEM. The one-way ANOVA and Duncan's post hoc tests was used for statistical analysis by SAS 9.1 (SAS Institute, USA). Graphs were generated by using GraphPad Prism 7.02 (GraphPad Software, USA). $P < 0.05$ indicated significant difference between the groups.

# Results

### Sodium oxalate inhibited cell proliferation activity and migration in MDCK cells

As shown in **Fig. 1A**, MDCK cells incubated with sodium oxalate for 24 h resulted in a decreased cell proliferation activity ($P < 0.05$) in a dose-dependent manner, compared with the control. Besides, the levels of LDH release in medium was significantly elevated in cells exposed to sodium oxalate treatment ($P < 0.05$) (**Fig. 1B**), indicating a loss of membrane integrity in response to sodium oxalate. Then, we performed a wound healing assay as shown in **Fig. 1C** and **1D** to evaluate the rate of cell migration. Treatment with sodium oxalate dose-dependently impeded the distance travelled by MDCK cells at 12 and 24 h ($P < 0.05$), suggesting that the cell migration rate was blocked by sodium oxalate.

### Sodium oxalate induced cell cycle arrest in MDCK cells

Compared with the control, sodium oxalate treatment increased the proportion of cells in G0/G1 phase and decreased the proportion of cells in S and G2/M phases ($P < 0.05$), suggesting that cell cycle shifted from S phase and G2/M phases toward G0/G1 phase (**Fig. 2A** and **2B**). EdU staining further verified the inhibition of sodium oxalate on cell proliferation (**Fig. 3A**). To confirm the cell proliferation at molecular level, mRNA level of genes involved in cell cycle was detected. As shown by RT-qPCR assay, cells incubated with sodium oxalate displayed a down-regulated mRNA level of proliferating cell nuclear antigen (PCNA) ($P < 0.05$). No significant difference was observed in terms of the mRNA level of cyclin D1 between sodium oxalate-treated MDCK cells and the control **(Fig. 3B)**.

### Sodium oxalate led to epithelial barrier dysfunction in MDCK cells

To explore the effect of sodium oxalate on epithelial barrier function, TEER and paracellular permeability of monolayer were measured, respectively. Following the exposure of cells to sodium oxalate, monolayer TEER was markedly reduced ($P < 0.05$) at 12, 24, 48 h **(Fig. 4A)**, in comparison with the control. Consistent with the decreased TEER in MDCK cells, 4 mmol/L of sodium oxalate treatment significantly increased the concentration of FITC-dextran ($P < 0.05$) in the basolateral of transwell insert at 12, 24, 48 h **(Fig. 4B)**, indicating an increase in paracellular permeability of monolayer.

### Sodium oxalate reduced tight junction proteins in MDCK cells

To investigate whether tight junction proteins are involved in sodium oxalate-induced epithelial barrier dysfunction, we examined the expression of tight junction proteins by RT-qPCR assay and Western blot. Compared with the control, cells exposure to sodium oxalate showed lower mRNA level of *claudin-1*, *occludin*, *ZO-1*, *ZO-2* and *ZO-3* ($P < 0.05$) than the control **(Fig. 5A)**. Likewise, the protein abundance of

tight junction proteins ($P < 0.05$), including claudin-1, occludin, ZO-1, ZO-2 and ZO-3, were prominently dose-dependently declined in response to sodium oxalate treatment **(Fig. 5B)**.

### Sodium oxalate repressed Wnt/β-catenin signaling in MDCK cells

Since Wnt/β-catenin signaling plays an vital role in the repair of injured renal tubular epithelial cells [13], we next detected the abundance of β-catenin and phosphorylated -β-catenin. As shown, compared with the control cells, sodium oxalate treatment led to decreased levels for β-catenin and p-β-catenin (Ser552) ($P < 0.05$) which are known as determinant markers for the activation of Wnt/β-catenin signaling **(Fig. 6A and 6B)**. Considering that cells treated with 4 mmol/L of sodium oxalate had reduced abundances for both β-catenin and p-β-catenin (Ser552) ($P < 0.05$), this concentration of sodium oxalate was used in the following experiments.

### Sodium oxalate-induced barrier dysfunction was reversed by GSK-3β inhibitor in MDCK cell

It has been reported that Wnt/β-catenin signaling regulates barrier function in vascular endothelial cells, especially in the blood-brain barrier [14]. To ascertain a functional role of Wnt/β-catenin signaling in cellular injury, MDCK cells were incubated with sodium oxalate in the presence or absence of GSK-3β inhibitor SB216763 (20 μmol/L), a specific agonist of Wnt/β-catenin signaling. Sodium oxalate-induced down-regulation of β-catenin and p-β-catenin (Ser552) were significantly reversed by SB216763 ($P < 0.05$), indicating Wnt/β-catenin signaling was reactivated by SB216763 **(Fig. 6C and 6D)**. Intriguingly, the decreased TEER of monolayer induced by sodium oxalate was alleviated by SB216763 ($P < 0.05$), compared with sodium oxalate treatment alone at 12, 24, 48 h **(Fig. 7A)**. Consistently, the elevated paracellular permeability in MDCK cells exposed to sodium oxalate was repressed by SB216763 treatment, as demonstrated by decreased concentration of FITC-dextran ($P < 0.05$) in the basolateral of transwell insert at 48 h **(Fig. 7B)**. These results indicated that Wnt/β-catenin signaling is critical for sodium oxalate-induced epithelial barrier dysfunction in MDCK cells. We next examined the effect of activation of Wnt/β-catenin on the sodium oxalate-induced reduction in the expression of TJ proteins by Western blot. As shown in **Fig. 7C** and **7D**, sodium oxalate treatment led to down-regulated protein abundance of claudin-1, occludin, ZO-1, ZO-2 and ZO-3, which was abrogated by SB216763 ($P < 0.05$).

## Discussion

Renal tubular epithelial cells is the pivotal cell type that participates in reabsorption and excretion, selectively transport nutrients and metabolic waste [15]. With aging of the companion animals, renal stone has become one of the most common diseases affecting the health of animals [16, 17]. However, the mechanism responsible for renal tubular epithelial cell injury during the development of stones has not been fully illuminated. High oxalate intake has been a key dietary factor actuating renal stone [18]. In the present study, we found that sodium oxalate treatment inhibited the proliferation and migration of MDCK cells by inducing cell cycle arrest. Importantly, a reduction in TEER and an increase in paracellular permeability were observed in sodium oxalate-treated epithelial cells, which is attributed to the decreased expression of tight junction proteins, including claudin-1, occludin, ZO-1, ZO-2, and ZO-3. These effects of

sodium oxalate were significantly blocked by GSK-3β inhibitor SB216763, indicating a critical role of Wnt/β-catenin signaling in sodium oxalate-induced barrier damage in MDCK cells.

Renal epithelial cells compensate for injured kidney through cell proliferation and migration. However, oxalate emerges as a factor inhibiting the proliferation of renal epithelial cells, which may exacerbate the progression of kidney disease. It has been reported that oxalate inhibits the viability of human proximal tubular epithelial cells in a dose- and time-dependent manner [19]. The mechanism by which oxalate inhibits the proliferation of rabbit renal proximal tubule cells has been relevant to oxidative stress, cPLA(2), p38 MAPK, and JNK signaling pathways [20]. A reduced cell proliferation activity and cell migration rate was observed in MDCK cells exposed to sodium oxalate in our study. Previous reports have shown that high concentrations of oxalate or calcium oxalate block the cell cycle progression in renal tubule epithelial cells from human and monkey [21, 22]. Consistently, our results indicated that sodium oxalate-treated MDCK cells displayed G1 phase cell cycle arrest, and a decreased cell population in the S and G2 phase. This result indicated that sodium oxalate inhibits cell growth in MDCK, at least in part, by triggering G1 arrest.

The transmembrane resistance of renal tubular epithelial cells is well-known indicator for the barrier integrity [23]. We found that sodium oxalate decreased the transmembrane resistance of MDCK monolayer cells in both dose- and time-dependent manner. In agreement with our study, result from Schepers et al. [24] corroborated that the transmembrane resistance presents a significant decrease in proximal renal tubular epithelial cells exposed to calcium oxalate crystals. In addition, sodium oxalate treatment results in a corresponding increase in the permeability of monolayer cells, indicating that sodium oxalate has a destructive effect on the barrier function of MDCK cells. The structural and functional integrity of the renal tubular epithelial cell barrier is extremely important for the reabsorption of water and nutrients and the maintaining of a stable internal environment. Oxygen free radicals is known to decrease the expression of tight junction protein in renal tubular epithelial cells [25]. In addition, exposure of MDCK cells to hydrogen peroxide significantly reduced the transmembrane resistance and the expression of tight junction proteins ZO-1 and occludin [26]. Peerapen et al. have demonstrated that calcium oxalate crystals decreased the expression of tight junction proteins ZO-1 and occludin by promoting the production of ROS and pro-inflammatory cytokines, which in turn leads to the destruction of the tight junctions of renal tubular epithelial cells [27].

In the present study, we found that sodium oxalate treatment decreased the expression of multiple tight junction proteins, including claudin-1, occludin, ZO-1, ZO-2, and ZO-3 in a dose-dependent manner at both transcriptional and protein levels. The tight junction proteins are inversely correlated to the paraepithelial cell permeability. Sodium oxalate reduced protein level of tight junction and contribute to the dysfunction of the barrier function of MDCK cells.

Studies have shown that Wnt/β-catenin signaling pathway is crucial for the formation and maintenance of tight junctions in endothelial cells [25, 28, 29]. Depletion of Apcdd1, one of the Wnt/β-catenin signaling pathway inhibitor, leads to an acceleration in barrier maturation of the retinal endothelial cells, which can

be rescued by overexpression of Apcdd1 [30]. *In vitro* study confirms an essential role of β-catenin signaling for the maintenance of the integrity of brain endothelial cells [28]. Despite these studies, the regulation of Wnt/β-catenin signaling on the tight junctions of renal tubular epithelial cells remains unknown. Our findings present a relevance of a blockage of β-catenin signaling with abnormally increased transmembrane resistance and reduced expression of claudin-1, occludin, ZO-1, ZO-2 and ZO-3 induced by sodium oxalate in MDCK cells. In contrast, these effects were reversed by activation of β-catenin, suggesting a protective role of Wnt/β-catenin in renal epithelial cell of canine

# Conclusions

In summary, our study revealed that sodium oxalate exposure led to reduced cell viability, G1 arrest in cell cycle progression, disruption of epithelial barrier integrity, and inhibition of Wnt/β-catenin signaling in MDCK cells. These effects of sodium oxalate were rescued by the presence of SB216763, a GSK-3β inhibitor, validating a critical role of Wnt/β-catenin singnalling and its contribution to sodium oxalate-induced renal epithelial injury. The data presented here provided scientific basis for the treatment of calcium oxalate-related renal stones in companion animals.

# Abbreviations

EdU: 5-Ethynyl-2'-deoxyuridine; GSK-3: glycogen synthase kinase-3; LDH; lactate dehydrogenase; MDCK: Mardin-Darby canine kidney; NaOx, sodium oxalate; PCNA, proliferating cell nuclear antigen; TEER, Trans epithelial electrical resistance; ZOs: zonula occludens.

# Declarations

### Availability of data and materials

Data and material sharing applicable to this article.


### Funding

This work was supported by the National Natural Science Foundation of China (No. 31625025), the Zhengzhou 1125 Talent Program, and the Jinxinnong Animal Science Development Foundation.


### Authors' contributions

The authors' responsibilities were as followed: ZW designed the research; SF, YJ,YY, and ZW analyzed the data; YJ, ZW, and SF wrote the paper. ZW had primary responsibility for final content. All authors read and approved the final version of the paper.

### Conflicts of Interest

The authors declare no conflict of interest.

### Consent for publication

Not applicable.

Ethics approval and consent to participate

Not applicable.

### Contributor Information

Yun Ji, Email: jean500@163.com

Shuting Fang, Email: caqdhfst@163.com

Ying Yang, Email: cauvet2020@hotmail.com

Zhenlong Wu, Phone: 86-10-62731003, Email: bio2046@hotmail.com

# References

1. Yasui T, Okada A, Hamamoto S, Ando R, Taguchi K, Tozawa K,et al. Pathophysiology-based treatment of urolithiasis. Int J Urol. 2017; 24(1): 32-38.
2. Syme HM. Stones in cats and dogs: What can be learnt from them? Arab J Urol. 2012; 10(3): 230-9.
3. Alford A, Furrow E, Borofsky M, Lulich J. Animal models of naturally occurring stone disease. Nat Rev Urol. 2020; 17(12): 691-705.
4. Wang Y, Zhou CJ, Liu Y. Wnt Signaling in Kidney Development and Disease. Prog Mol Biol Transl Sci. 2018; 153: 181-207.
5. Gunzel D, Yu AS. Claudins and the modulation of tight junction permeability. Physiol Rev. 2013; 93(2): 525-69.
6. Steinhart Z, Angers S. Wnt signaling in development and tissue homeostasis. Development. 2018; 145(11).
7. Ponce DP, Maturana JL, Cabello P, Yefi R, Niechi I, Silva E,et al. Phosphorylation of AKT/PKB by CK2 is necessary for the AKT-dependent up-regulation of β-catenin transcriptional activity. J Cell Physiol. 2011; 226(7): 1953-9.
8. Stamos JL, Weis WI. The beta-catenin destruction complex. Cold Spring Harb Perspect Biol. 2013; 5(1): a007898.
9. Gewin LS. Renal Tubule Repair: Is Wnt/β-Catenin a Friend or Foe? Genes (Basel). 2018; 9(2).
10. Nusse R, Clevers H. Wnt/β-Catenin Signaling, Disease, and Emerging Therapeutic Modalities. Cell. 2017; 169(6): 985-99.
11. Malik SA, Modarage K, Goggolidou P. The Role of Wnt Signalling in Chronic Kidney Disease (CKD). Genes (Basel). 2020; 11(5).

12. Zhou D, Tan RJ, Fu H, Liu Y. Wnt/beta-catenin signaling in kidney injury and repair: a double-edged sword. Lab Invest. 2016; 96(2): 156-67.
13. Zhou L, Liu Y. Wnt/β-catenin signaling and renin-angiotensin system in chronic kidney disease. Curr Opin Nephrol Hypertens. 2016; 25(2): 100-6.
14. Cong X, Kong W. Endothelial tight junctions and their regulatory signaling pathways in vascular homeostasis and disease. Cell Signal. 2020; 66: 109485.
15. Blanchard A, Poussou R, Houillier P. [Exploration of renal tubular functions]. Nephrol Ther. 2009; 5(1): 68-83.
16. O'Kell AL, Grant DC, Khan SR. Pathogenesis of calcium oxalate urinary stone disease: species comparison of humans, dogs, and cats. Urolithiasis. 2017; 45(4): 329-36.
17. Hunprasit V, Schreiner PJ, Bender JB, Lulich JP. Epidemiologic evaluation of calcium oxalate urolithiasis in dogs in the United States: 2010-2015. J Vet Intern Med. 2019; 33(5): 2090-95.
18. Marsh BM, Sathianathen N, Tejpaul R, Albersheim-Carter J, Bearrick E, Borofsky MS. Public Perceptions on the Influence of Diet and Kidney Stone Formation. J Endourol. 2019; 33(5): 423-29.
19. Bhandari A, Koul S, Sekhon A, Pramanik SK, Chaturvedi LS, Huang M,et al. Effects of oxalate on HK-2 cells, a line of proximal tubular epithelial cells from normal human kidney. J Urol. 2002; 168(1): 253-9.
20. Han HJ, Lim MJ, Lee YJ. Oxalate inhibits renal proximal tubule cell proliferation via oxidative stress, p38 MAPK/JNK, and cPLA2 signaling pathways. Am J Physiol Cell Physiol. 2004; 287(4): C1058-66.
21. Han J, Guo D, Sun XY, Wang JM, Ouyang JM, Gui BS. Repair Effects of Astragalus Polysaccharides with Different Molecular Weights on Oxidatively Damaged HK-2 Cells. Sci Rep. 2019; 9(1): 9871.
22. Sun XY, Yu K, Ouyang JM. Time-dependent subcellular structure injuries induced by nano-/micron-sized calcium oxalate monohydrate and dihydrate crystals. Mater Sci Eng C Mater Biol Appl. 2017; 79: 445-56.
23. Srinivasan B, Kolli AR, Esch MB, Abaci HE, Shuler ML, Hickman JJ. TEER measurement techniques for in vitro barrier model systems. J Lab Autom. 2015; 20(2): 107-26.
24. Schepers MS, van Ballegooijen ES, Bangma CH, Verkoelen CF. Crystals cause acute necrotic cell death in renal proximal tubule cells, but not in collecting tubule cells. Kidney Int. 2005; 68(4): 1543-53.
25. Peerapen P, Thongboonkerd V. p38 MAPK mediates calcium oxalate crystal-induced tight junction disruption in distal renal tubular epithelial cells. Sci Rep. 2013; 3: 1041.
26. Bilal S, Jaggi S, Janosevic D, Shah N, Teymour S, Voronina A,et al. ZO-1 protein is required for hydrogen peroxide to increase MDCK cell paracellular permeability in an ERK 1/2-dependent manner. Am J Physiol Cell Physiol. 2018; 315(3): C422-C31.
27. Peerapen P, Thongboonkerd V. Effects of calcium oxalate monohydrate crystals on expression and function of tight junction of renal tubular epithelial cells. Lab Invest. 2011; 91(1): 97-105.

28. Tran KA, Zhang X, Predescu D, Huang X, Machado RF, Gothert JR,et al. Endothelial beta-Catenin Signaling Is Required for Maintaining Adult Blood-Brain Barrier Integrity and Central Nervous System Homeostasis. Circulation. 2016; 133(2): 177-86.
29. Laksitorini MD, Yathindranath V, Xiong W, Hombach-Klonisch S, Miller DW. Modulation of Wnt/beta-catenin signaling promotes blood-brain barrier phenotype in cultured brain endothelial cells. Sci Rep. 2019; 9(1): 19718.
30. Mazzoni J, Smith JR, Shahriar S, Cutforth T, Ceja B, Agalliu D. The Wnt Inhibitor Apcdd1 Coordinates Vascular Remodeling and Barrier Maturation of Retinal Blood Vessels. Neuron. 2017; 96(5): 1055-69 e6.

# Figures

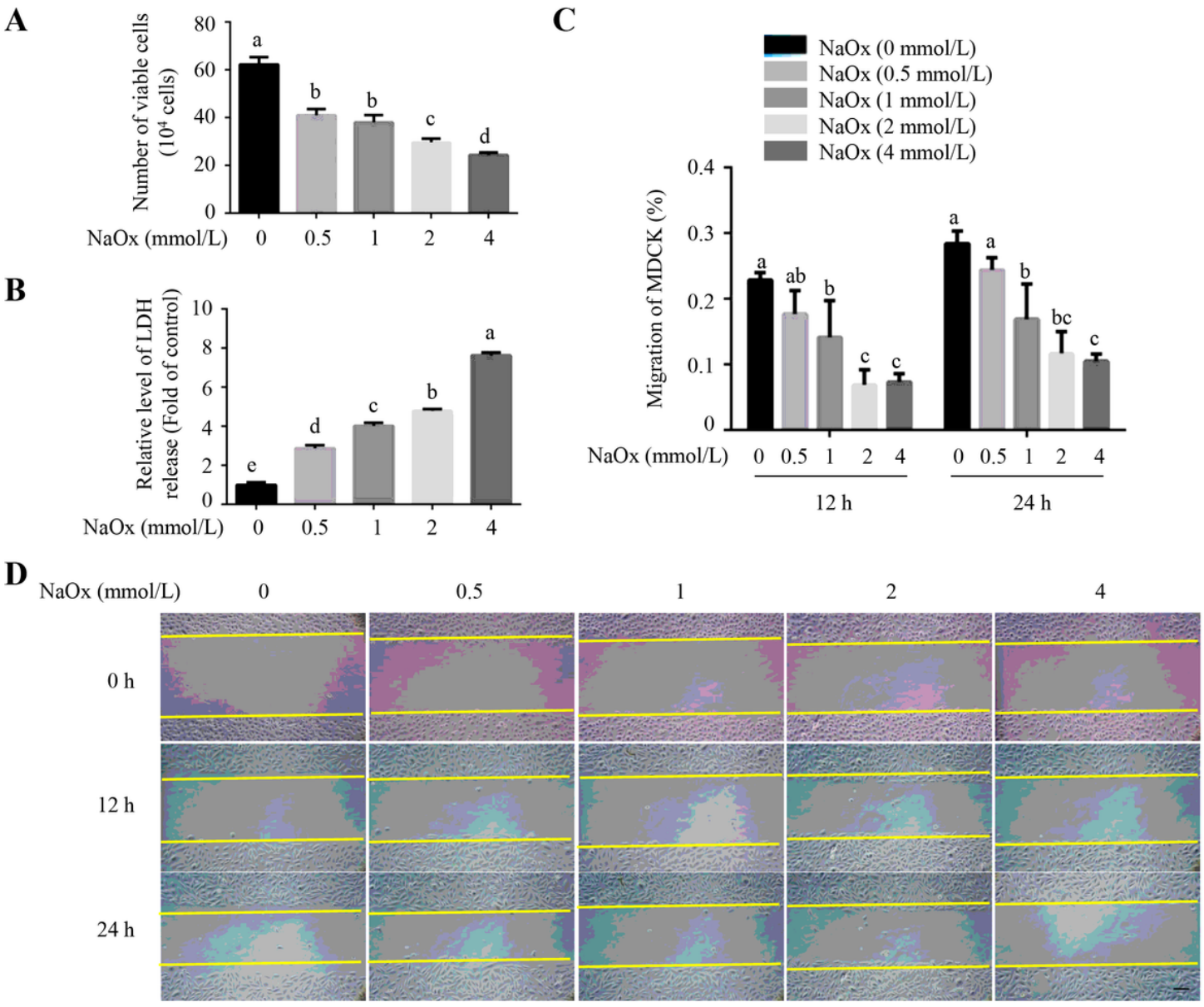


Figure 1

Effect of sodium oxalate exposure on proliferation activity of MDCK cells. (A) Cells were treated with various doses (0, 0.5, 1, 2, 4 mmol/L) of sodium oxalate for 24 h, followed by a determination of cell proliferation activity assessed by trypan blue staining. (B) The activity of lactate dehydrogenase (LDH) released into medium from cell treated with sodium oxalate for 24 h were detected. (C and D) Following treatment with sodium oxalate for 24 h, the confluent monolayers were wounded with pipette tips. The cell migration rate was recorded at 0, 12, and 24 h, respectively. Images are representative of three observations. Scale bar indicates 50 μm. Values are means ± SEM. n = 3. Means without common superscripts differ ($P < 0.05$). NaOx, sodium oxalate.

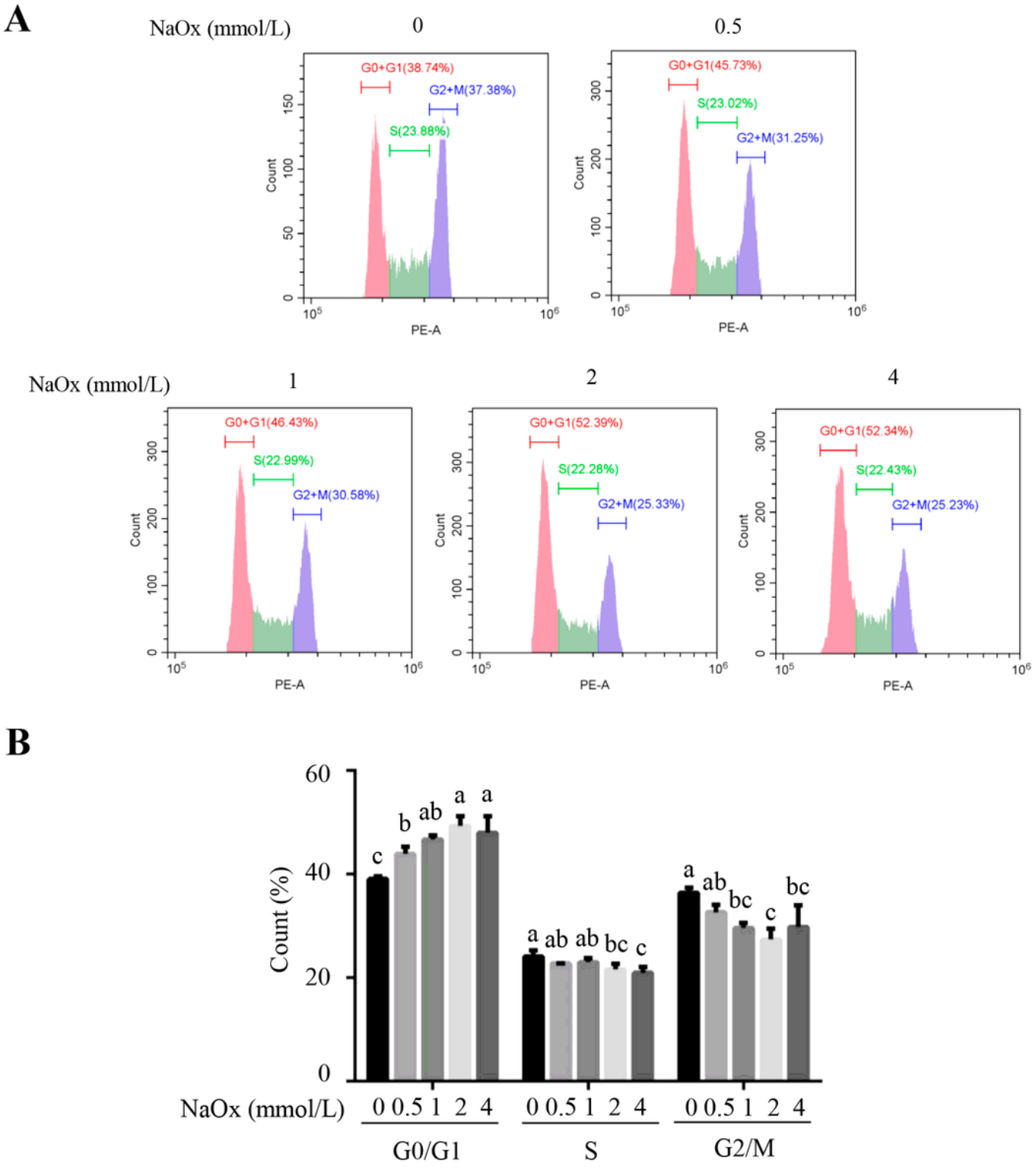


## Figure 2

Cell cycle analysis of MDCK cells exposed to sodium oxalate treatment. (A) MDCK cells were subjected to a 6 h serum starvation and then a 24 h treatment of sodium oxalate, following which cell cycle distribution were measured by flow cytometry. (B) Percentage of MDCK cells in G0/G1, S, and G2/M phases. Data are presented as means ± SEM. n = 3. Bars labeled with a different letter mean significant difference ($P < 0.05$). NaOx, sodium oxalate.

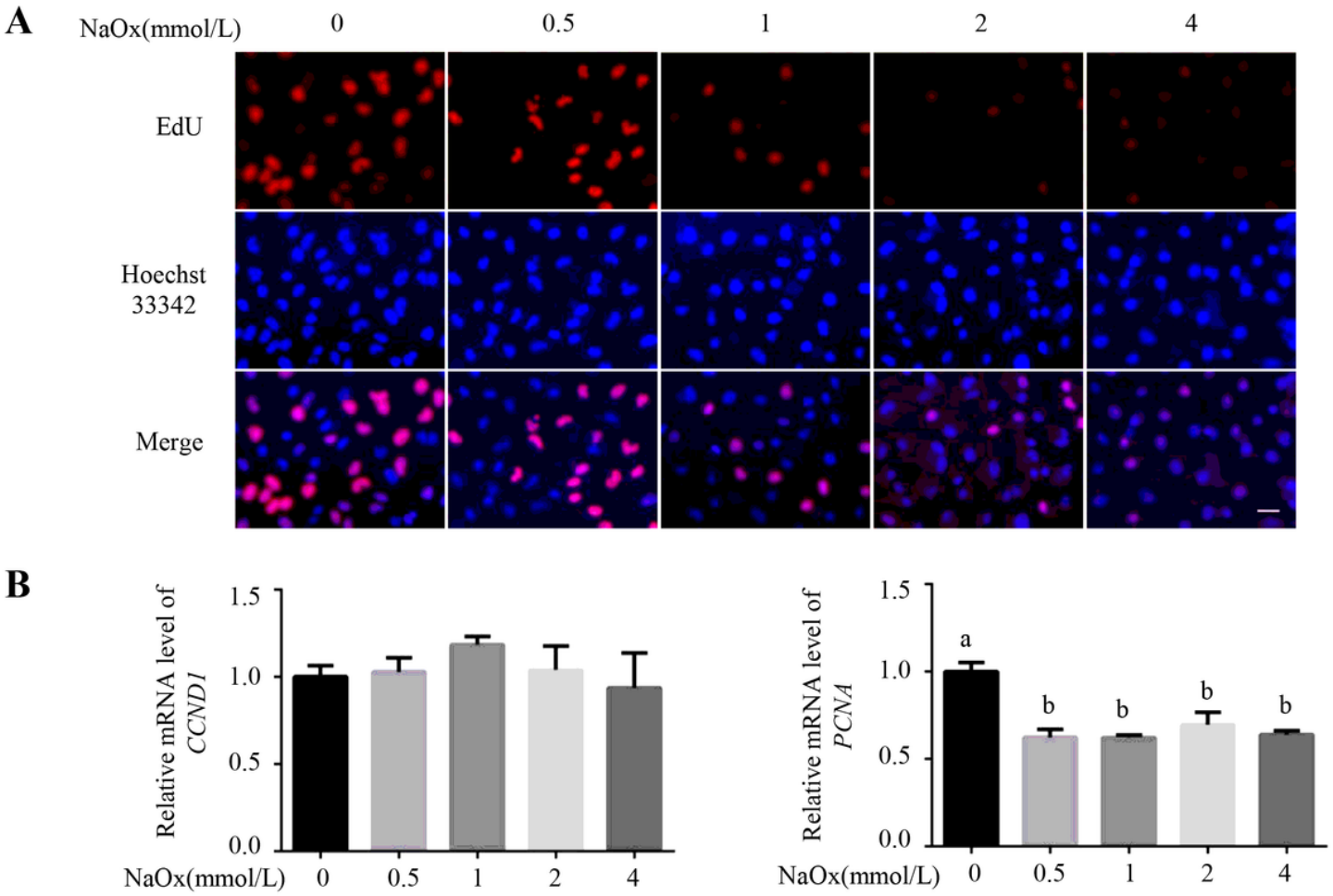


## Figure 3

Sodium oxalate-induced stagnation in cell proliferation evaluated by EdU assay and cell cycle-related gene expression. (A) MDCK cells were allowed to proliferate for 24 h in the present of different concentrations of sodium oxalate, followed by an EdU and Hoechst 33342 staining. Scale bar: 20 μm. (B) Cells were treated with sodium oxalate for 24 h before RNA extraction, after which RT-qPCR were performed to detect the relative mRNA level of CCND1 and PCNA. GAPDH was used as a reference gene. n = 3. Means without a common letter differ ($P < 0.05$). NaOx, sodium oxalate.

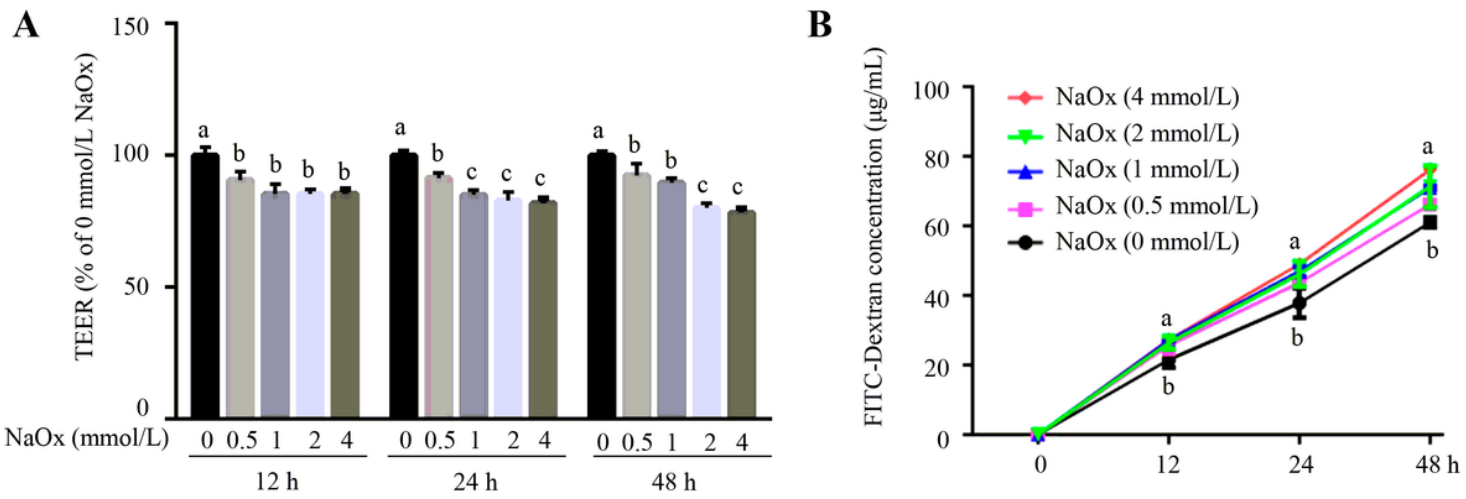


## Figure 4

Effect of sodium oxalate treatment on barrier function of MDCK cells. Cells were subjected to sodium oxalate for up to 48 h, during which transepithelial electric resistance (TEER) (A), and (B) paracellular permeability were determined. Values are shown as mean ± SEM, n = 3. Different letters represent significant differences ($P < 0.05$). NaOx, sodium oxalate; TEER, transepithelial electrical resistance; FITC, fluorescein isothiocyanate.

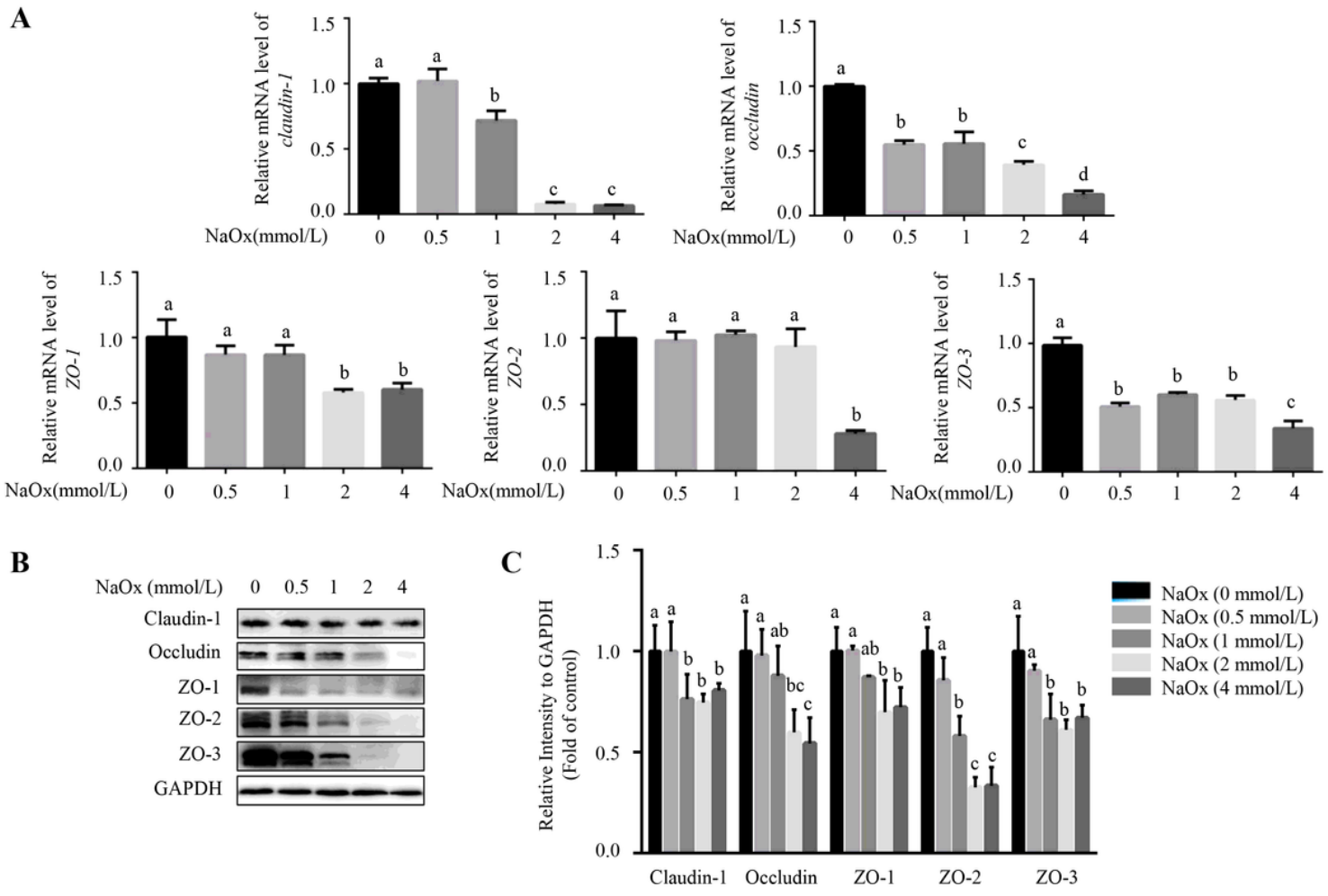

## Figure 5

Addition of sodium oxalate inhibits the expression of tight junction protein at both transcriptional and protein level. Cells treated with 0, 0.5, 1, 2, and 4 mmol/L of sodium oxalate for 24 h were harvested for RT-qPCR (A) or Western blot analysis (B). GAPDH was regarded as a reference gene or loading control. n = 3. Means without a common letter differ (P < 0.05). NaOx, sodium oxalate.

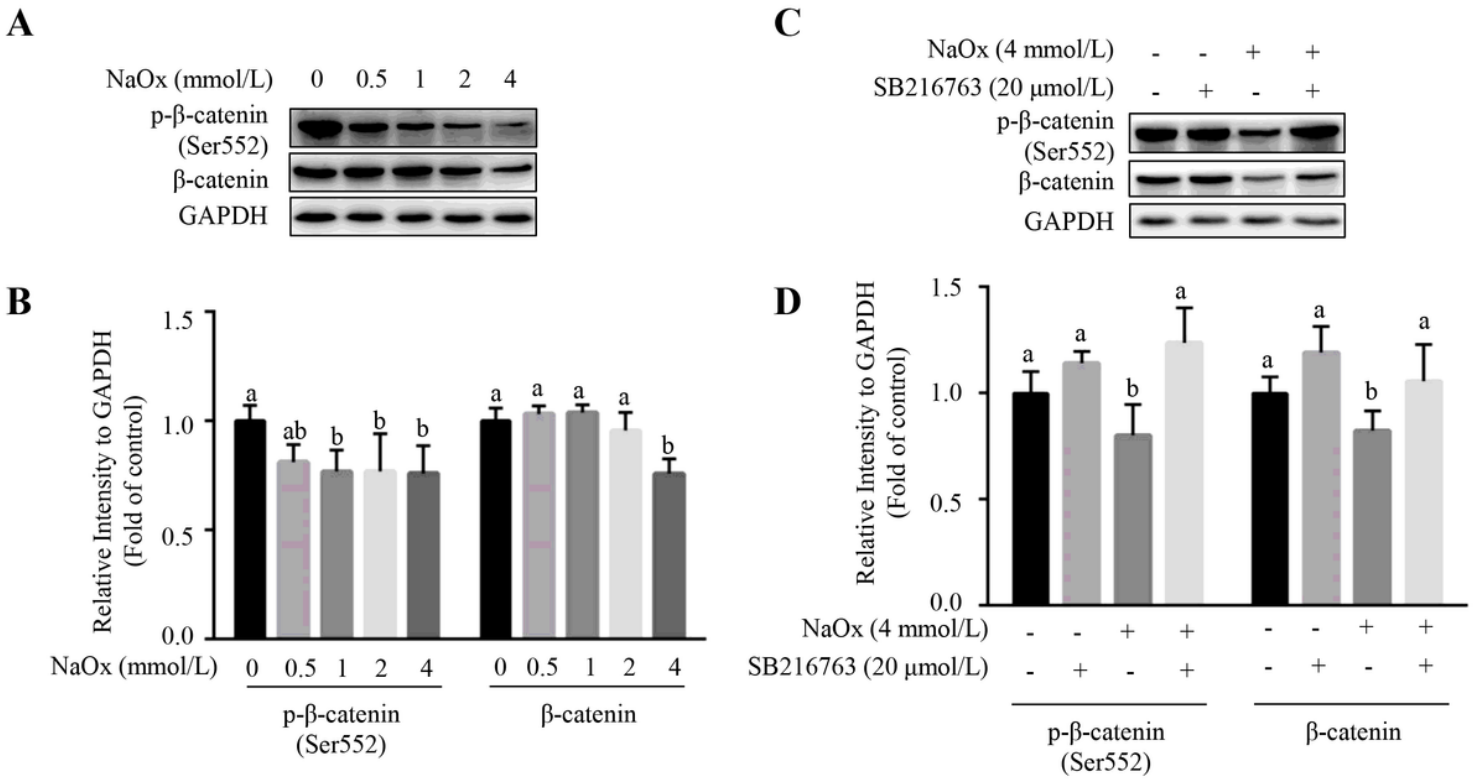


## Figure 6

GSK3β inhibitor (SB216763) blocks sodium oxalate-induced decease in the levels of p-β-catenin (Ser552) and β-catenin. (A) MDCK cells were challenged with various concentrations of sodium oxalate for before Western blot analysis. (B) The reduction in the protein abundance of p-β-catenin (Ser552) and β-catenin was impeded in the presence of SB216763. n = 3. Bars without a common letter denote significant difference (P < 0.05). NaOx, sodium oxalate.

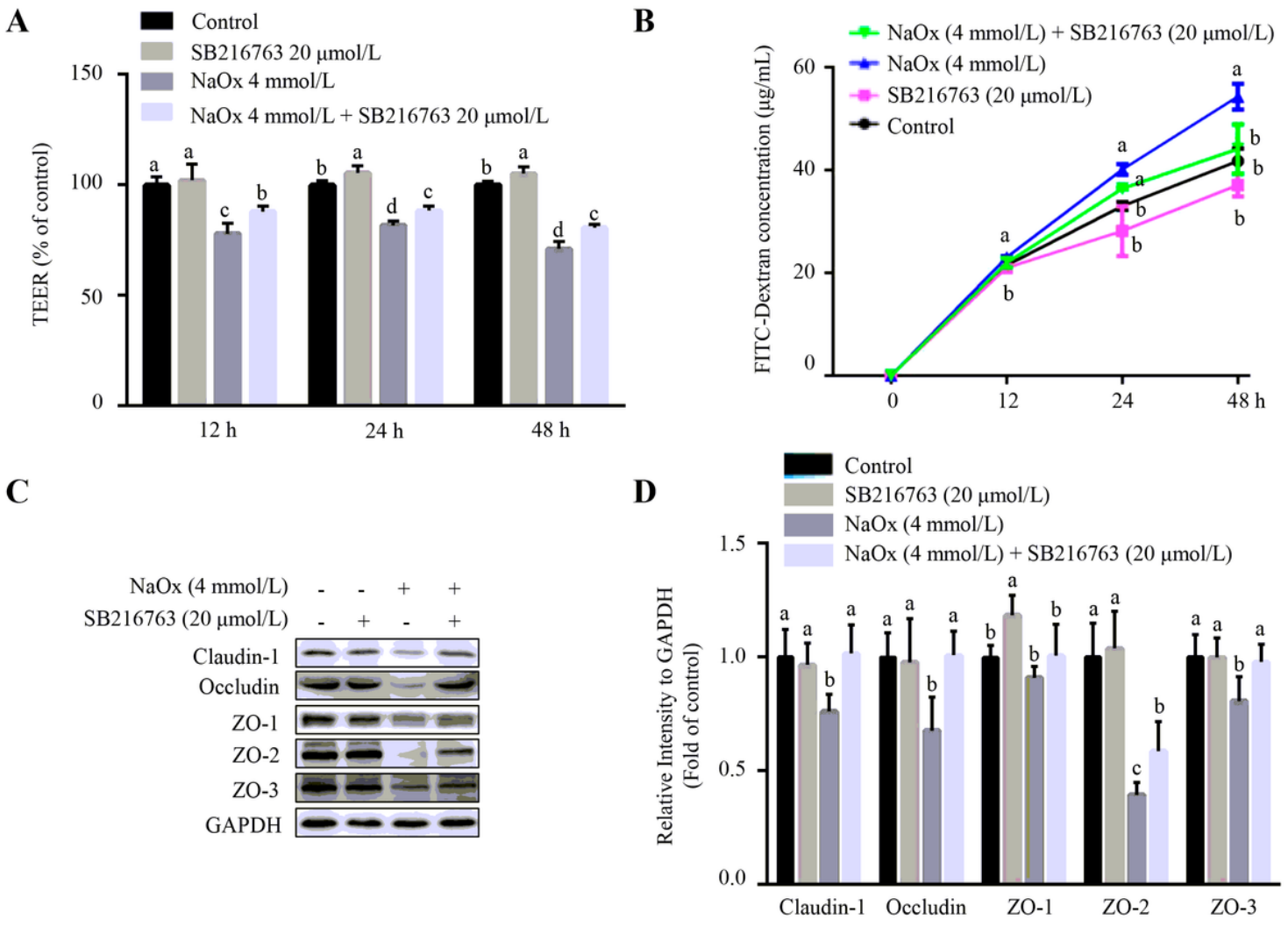


**Figure 7**

Sodium oxalate-induced disruption in barrier function of MDCK cells is revered by treatment of SB216763. (A) TEER measurement of MDCK monolayer treated with sodium oxalate in the presence or absence of SB216732. (B) Evaluation of paracellular permeability by FITC-Dextran assay. (C and D) Western blot analysis of tight junction proteins (claudin-1, occluding, ZO-1, ZO-2, and ZO-3) in MDCK cells exposed to sodium oxalate, SB216763 or sodium oxalate in combination with SB216763 treatment. n = 3. FITC, fluorescein isothiocyanate; NaOx, sodium oxalate; TEER, transendothelial electrical resistance. Means with no common letters indicate significantly different ($P < 0.05$).

# Supplementary Files

This is a list of supplementary files associated with this preprint. Click to download.

- renamed6dbb3.docx